Available online at www.derpharmachemica.com

ISSN 0975-413X
CODEN (USA): PCHHAX

Der Pharma Chemica, 2016, 8(5):147-155
(http://derpharmachemica.com/archive.html)

Pharmacophore Modelling, Atom- and Field-based 3D QSAR Studies of Cytotoxic Acridones Derivatives

G. Deepak Reddy[1], Y. Rajesh Babu[2], B. S. Sastry[2] and V. V. S. R. Prasad[1]

[1]*Medicinal Chemistry Research Division, Vishnu Institute of Pharmaceutical Education and Research, Narsapur, India*
[2]*Department of Pharmaceutical Chemistry, Gland Institute of Pharmaceutical Sciences, Narsapur, India*

ABSTRACT

In the current investigations, we have identified an efficient pharmacophore from a set of 38 acridones that are earlier proved to possess moderate to high cytotoxic activity against HL-60 cancer cells. We have deployed two diverged QSAR analyses such as Atom-based and Field-based QSAR techniques by employing Partial Least Square regression analysis in order to elucidate the structural insights of acridones. Identified pharmacophoric features such as one hydrogen bond acceptor, one hydrophobic region, three aromatic rings i.e, AHRRR. Regression analyses of Atom-based 3D-QSAR models resulted with regression coefficients of r^2 of 0.98 and q^2 of 0.74, and Pearson-R of 0.92. Gaussian-based 3D QSAR studies revealed that larger alkyl group along with Nitrogen atom of secondary amine at N10-position and carbonyl oxygen of acridone nucleus as favourable regions for the cytotoxic activity. Regression scores of Gaussian-based QSAR model showed that regression coefficients of r^2 of 0.92 and q^2 of 0.68, and Pearson-R of 0.84.

Keywords: Acridones, HL-60, Pharmacophore model, 3D QSAR, Field-based QSAR

INTRODUCTION

Acridones are the alkaloid class phytoconstituents majorly isolated from members of *Rutaceae* family. [1]. Earlier research proved diverged effects of acridones including antibacterial, antimalarial activities [2,3,]. A number of acridone derivatives are also reported for their potent in vitro anticancer activity, including modulation of multidrug resistance in cancer cells [4-7]. The *in vitro* antiproliferative and anticancer activities of acridones was proved against several cancer cell lines [8,9].Natural compounds such as acronycine and glyfoline possess significantly potent in vitro cytotoxic activity, particularly against human leukaemia HL-60 cells [10,11].In our earlier publications, we have reported a wide spectrum of acridone derivatives with different substitutions such as N10-alkylation, and halo-acridone moieties possessing potential cytotoxic activity against both drug sensitive and resistant human leukaemia HL-60 cells [12, 13, 14]. In the current study, we have focused on the structural insights of the acridones for their cytotoxic activity against HL-60 cells by identifying efficient common pharmacophore model from the defined set of acridones and from which an Atom-based 3D-QSAR model has been derived. Additionally, we have also elucidated the steric and electrostatic fields of acridones with respect to the Hl-60 cytotoxicity through Field-based QSAR studies.

MATERIALS AND METHODS

Data set ligands:
A set of 38 N^{10}-substituted acridone derivatives which were previously designed, synthesized in our laboratory and screened for their *in-vitro* cytotoxic effects (pIC_{50}) against doxorubicin resistant HL-60 cell lines (HL-60), results thus obtained were selected for the present study **[**12,13, 14]. The data set consists of inactive, intermediate and

highly active molecules. Out of 38 molecules, 80 % were randomly selected as training set and remaining as test set for QSAR analysis. 2D molecular structures of the ligands were shown in **Table 1.**

Table: 1: Structures of selected acridone derivatives

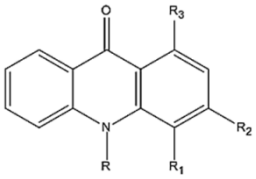

Compound No	R	R1	R2	R3
1	-H	F	H	H
2	-CH_2-CH_2-CH_2-Cl	F	H	H
3	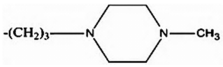	F	H	H
4	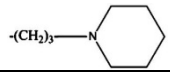	F	H	H
5	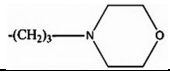	F	H	H
6	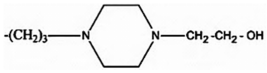	F	H	H
7	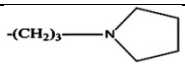	F	H	H
8	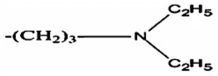	F	H	H
9	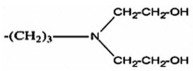	F	H	H
10	-CH_2-CH_2-CH_2-CH_2-Cl	F	H	H
11	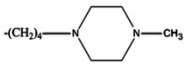	F	H	H
12	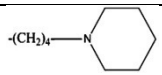	F	H	H
13	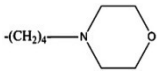	F	H	H
14	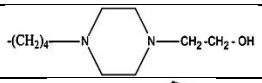	F	H	H
15	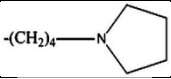	F	H	H
16	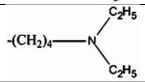	F	H	H
17	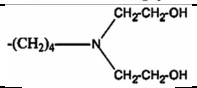	F	H	H
18	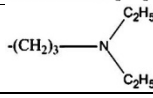	Cl	H	H

19	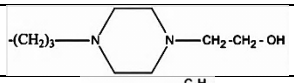	Cl	H	H
20	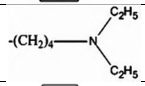	Cl	H	H
21	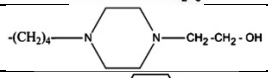	Cl	H	H
22	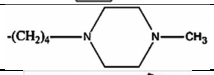	Cl	H	H
23	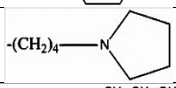	Cl	H	H
24	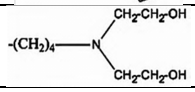	Cl	H	H
25	$-CH_2-CH_2-CH_2-Cl$	H	$COOCH_3$	$COOCH_3$
26	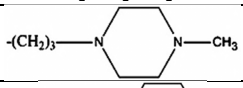	H	$COOCH_3$	$COOCH_3$
27	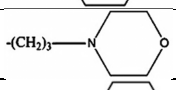	H	$COOCH_3$	$COOCH_3$
28	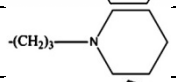	H	$COOCH_3$	$COOCH_3$
29	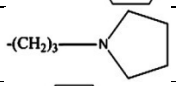	H	$COOCH_3$	$COOCH_3$
30	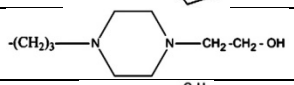	H	$COOCH_3$	$COOCH_3$
31	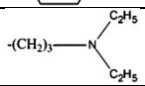	H	$COOCH_3$	$COOCH_3$
32	$-CH_2-CH_2-CH_2-CH_2-Cl$	H	$COOCH_3$	$COOCH_3$
33	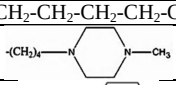	H	$COOCH_3$	$COOCH_3$
34	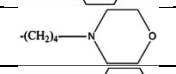	H	$COOCH_3$	$COOCH_3$
35	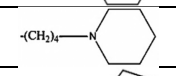	H	$COOCH_3$	$COOCH_3$
36	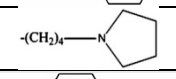	H	$COOCH_3$	$COOCH_3$
37	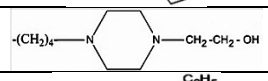	H	$COOCH_3$	$COOCH_3$
38	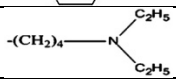	H	$COOCH_3$	$COOCH_3$

Ligand Preparation:

Molecules selected for the analysis were designed using Chem Sketch of Schrodinger suite 2012 and then subjected to geometrical optimization using Ligprep module. In this step, a single, low energy 3D structure was obtained for each ligand and many conformers/tautomers obtained during ionization of the ligands using EPIK module which generate ionization states at pH range of 7±2 [15].

Pharmacophore development and QSAR analysis:

Common pharmacophore hypotheses (CPH) and 3D-QSAR models were generated by using Phase module of Schrodinger suite for the set of 38 acridone containing ligands selected from the previously published results from our laboratory [16]. All the ligands were categorized into active, intermediate and inactive according to the activity thresholds. To generate common pharmacophore hypotheses, maximum of six sites were selected in order to obtain an efficient model. The Phase activity provides a six set pharmacophoric features, hydrogen bond acceptor (A), hydrogen bond donor (D), hydrophobic group (H), positively ionizable (P), negatively ionizable (N), and aromatic ring (R). Hypotheses were generated by a systematic variation of number of sites (n_{sites}) and the number of matching active compounds (n_{act}). With $n_{act} = n_{act - tot}$ initially ($n_{act - tot}$) is the total number of active compounds in the training set, n_{sites}.

Atom- and Field-Based QSAR Studies

Atom based QSAR model has been developed based on the obtained pharmacophore models and by maintaining 1.00Å and six partial least squares (PLS) factors. Whereas, Field-based QSAR tool of Schrodinger Suite was used to develop Gaussian-based QSAR models. Cytotoxic activity of 38 ligands from the Data set against the HL60 human leukemia cancer cell line was considered for building a QSAR model. Parameters such as performed using Gaussian based steric, electrostatic, hydrophobic, hydrogen bond donor (HBD) and hydrogen bond acceptor (HBA) potential fields were calculated accordingly. For PLS regression analysis, pIC_{50} values of the molecules are considered as dependent variable and Guassian intensities are considered as independent variable. QSAR model was built and calculated by constructing with a 3D cubic lattice with 1Å grid spacing, and can be extended by 3Å beyond training set limits. Energies cutoff was set to ±30 kcal/mol and the variable with standard deviation with <0.01 were eliminated[17].

Eighty percent of the data set molecules were randomly selected as training set. Upto six PLS factors were generated for atom- and field- based models and the models. The obtained models were validated by predicting the activity of test set ligands.

The predictive value of the models was evaluated by leave one-out (LOO) and leave-half-out (LHO) cross-validation. The cross-validated coefficient (r^2_{cv}) was calculated using the following equation:

$$r_{cv}^2 = 1 - \frac{\Sigma(Y_{predicted} - Y_{observed})^2}{\Sigma(Y_{observed} - Y_{mean})^2} \quad (1)$$

Here $Y_{predicted}$, $Y_{observed}$, and Y_{mean} are the predicted, observed and mean values of the target property (pIC_{50}) respectively. $(Y_{observed} - Y_{mean})^2$ is the predictive residual sum of squares (PRESS). The predictive correlation coefficient (r^2_{pred}) based on molecules of the test set, is defined as,

$$r_{pred}^2 = \frac{SD - PRESS}{SD} \quad (2)$$

where SD is the sum of the squared deviation between the biological activities of the test set and mean activities of the training set molecules, PRESS is the sum of squared deviation between predicted and actual activity values for every molecule in the test set. According to the literature, 3D-QSAR models accepted if [18]

$R^2 > 0.6$; R^2_{cv} (Q^2) > 0.5 (3)

RESULTS AND DISCUSSION

We have divided the selected 38 molecules into active ($pIC_{50} > 4.9$), intermediate (pIC_{50} = 4.9-4.7) and inactive ($pIC_{50} > 4.7$) for the identification and development of an efficient common pharmacophore responsible for cytotoxicity against HL60 cancer cells. For the 38 ligands, a total of 8 common pharmacophoric hypotheses with five pharmacophoric features were identified, AHRRR, one hydrogen bond acceptor (A), one hydrophobic group (H), and three aromatic rings (R). Despite similar pharmacophoric features, the 3D spatial arrangements of the pharmacophoric features were different. Spatial arrangement of AHRRR.23 pharmacophoric hypothesis is shown in **Figure 1**.

QSAR models for the obtained CPHs were built to identify the better pharmacophore model. Survival scores of the obtained CPHS were ranging between 3.318 (AHRRR.23) and 2.756 (APRRR.2).The highest regression scores of r^2 0.98, q^2 of 0.74 and Pearson-R of 0.92 were resulted through Atom-based QSAR for AHRRR.23hypothesis by using Partial least square analysis. Alignment of the molecules onto developed pharmacophore AHRRR.23is shown in **Figure 2.**The QSAR regression analysis plots of actual activity (phase activity) vs predicted activity is shown in **Figure 3** for training ligands and for test ligands (inset).

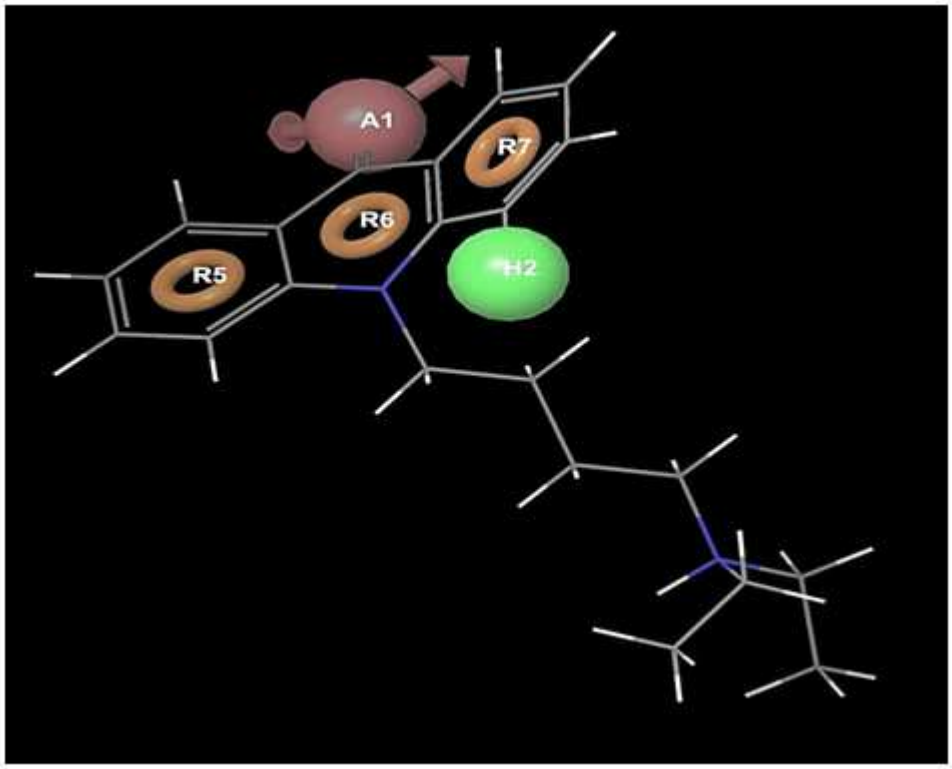

Figure 1: 3D spatial arrangement of the common pharmacophore AHRRR.23

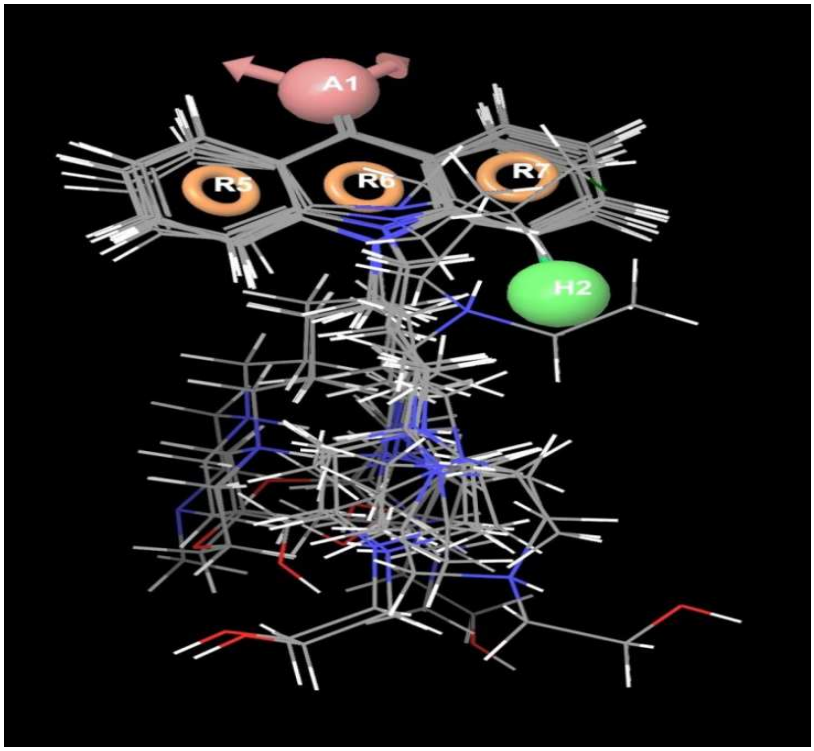

Figure 2: Ligand based alignment of the data set molecules

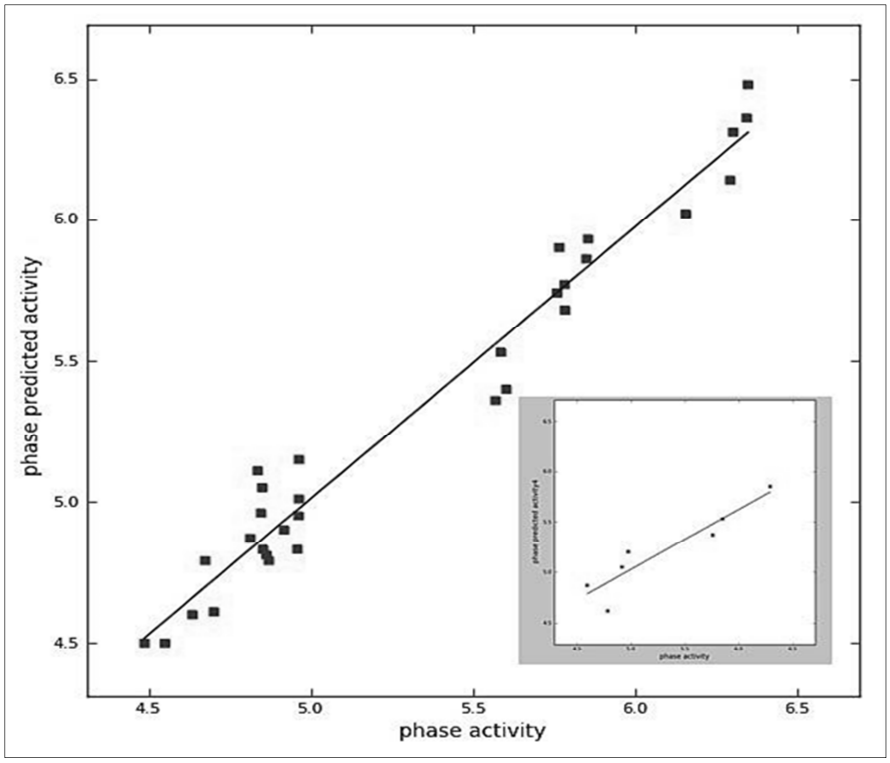

Figure 3: QSAR Plots of predicted vs actual pIC_{50} for training set ligands and test set ligands (inset)acridones obtained from Atom-based QSAR

The Gaussian steric and electrostatic field contour plots obtained from multifit alignment employing independent variables of compounds with highest and least cytototoxic activities are shown in **Figure 4 and 5.**QSAR visualization through Contour mapping includes magenta (favoured) and red contours (disfavoured) for steric parameter, the hydrogen bond donor fields are indicated by purple (favoured) denote hydrogen bond acceptor fields and cyan (disfavoured), the hydrophobic fields represented by yellow (favoured) and white (disfavoured). The electrostatic fields are represented by red- (electronegative group favoured) and blue-colored contours (electropositive group favoured), and the steric fields are represented by green (bulky substitution favoured) and yellow-colored contours (bulky substitution disfavoured). The statistical parameters and the field fractions calculated in Gaussian based QSAR are tabulated in **Table 2**. Variables such as steric, hydrophobic, and H-bond acceptor were identified as the major constituents of the cytotoxicity activity of the compounds. Regression analysis resulted in higher regression coefficient (r^2) value of 0.92 for the training set, q^2 of 0.68, cross-validated correlation coefficient (r^2_{cv}) of 0.77 and Pearson-R of 0.84.The actual and predicted pIC_{50} values of the dataset ligands for Gaussian based model are shown in **Figure 6**.

Table 2: Statistical parameters and the field fractions in Gaussian based QSAR

#Factor	QSAR Statistics				Field Fractions (Gaussian)				
	R^2	F	Q^2	Pearson-R	Steric	Electrostatic	Hydrophobic	H bond Acceptor	H bond Donor
1	0.61	32.1	0.58	0.69	0.4041	0.0995	0.3009	0.1484	0.0448
2	0.70	34.9	0.61	0.71	0.3639	0.1165	0.2915	0.1651	0.0631
3	0.73	40.4	0.69	0.79	0.3554	0.1292	0.2789	0.1653	0.0713
4	0.86	43.8	0.67	0.87	0.3226	0.1403	0.2831	0.1745	0.0795
5	0.92	55.1	0.68	0.84	0.3124	0.1345	0.2817	0.1810	0.0804

CONCLUSION

In the present study, the most suitable common pharmacophore from the acridone derivatives was identified, which consisting of 5 pharmacophore features with one hydrogen bond acceptor, one hydrophobic group, and tricyclic aromatic rings (AHRRR). Presence of the larger alkyl group at N^{10}-position of acridone nucleus and nitrogen containing substituted side chain was identified as the favourable region for the cytotoxicity against HL-60 cancer cells. This is also supported by the Gaussian models obtained through the Field-based QSAR studies deployed to identify the favourable and dis-favoured regions of acridone derivatives. We propose that the derived 3D-QSAR models provide possible structural insights and aid the strategic design of molecules with improved cytotoxic potentials.

Acknowledgements
We wish to acknowledge Sri Vishnu Educational Society (SVES) for the providing research facilities. We would also like to thank Schrodinger, USA for providing us academic evaluation to carry out research.

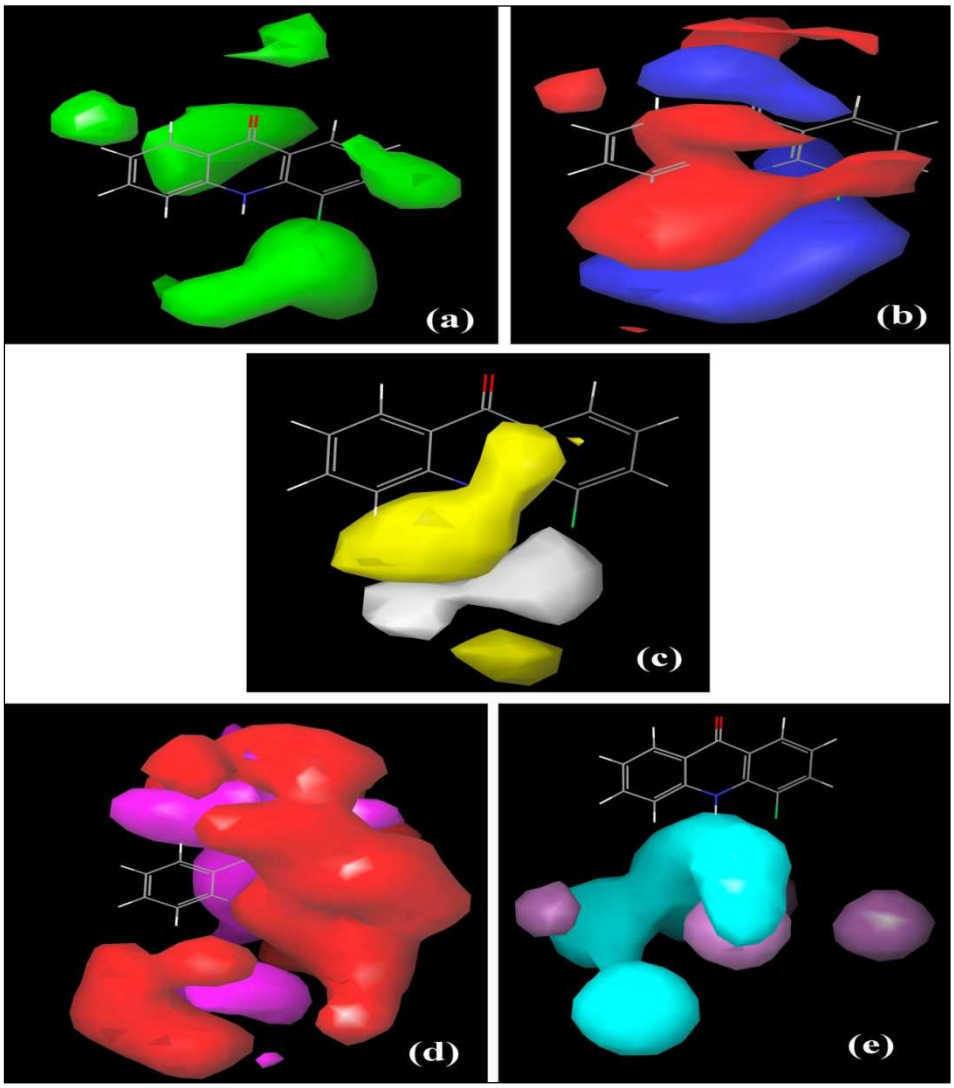

Figure 4: Contour mapping of the Field-based (Gaussian) QSAR for compound with highest activity

a) steric (green is positive); b) electrostatic (blue is positive and red is negative); c) Hydrophobic (yellow is positive and white is negative); d) Hydrogen bond acceptor (red is positive and magenta is negative); e) H-bond donor (purple is positive and cyan is negative)

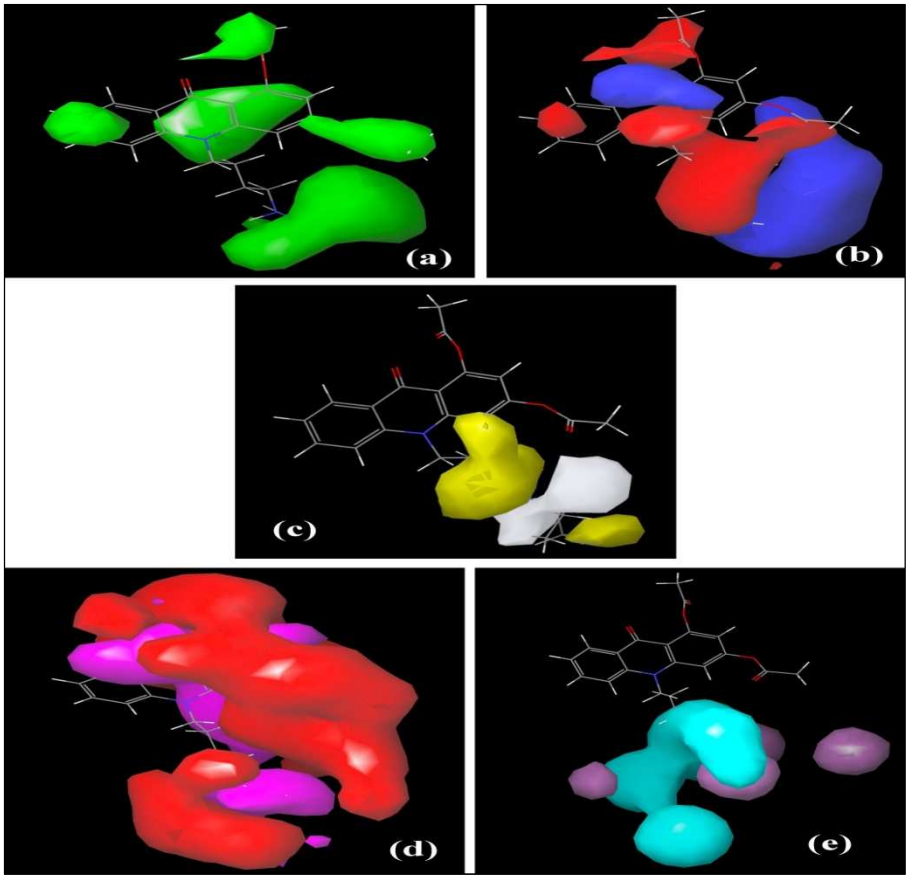

Figure 5: Contour mapping of the Field-based (Gaussian) QSAR for compound with lowest activity

a) steric (green is positive); b) electrostatic (blue is positive and red is negative); c) Hydrophobic (yellow is positive and white is negative); d) Hydrogen bond acceptor (red is positive and magenta is negative); e) H-bond donor (purple is positive and cyan is negative)

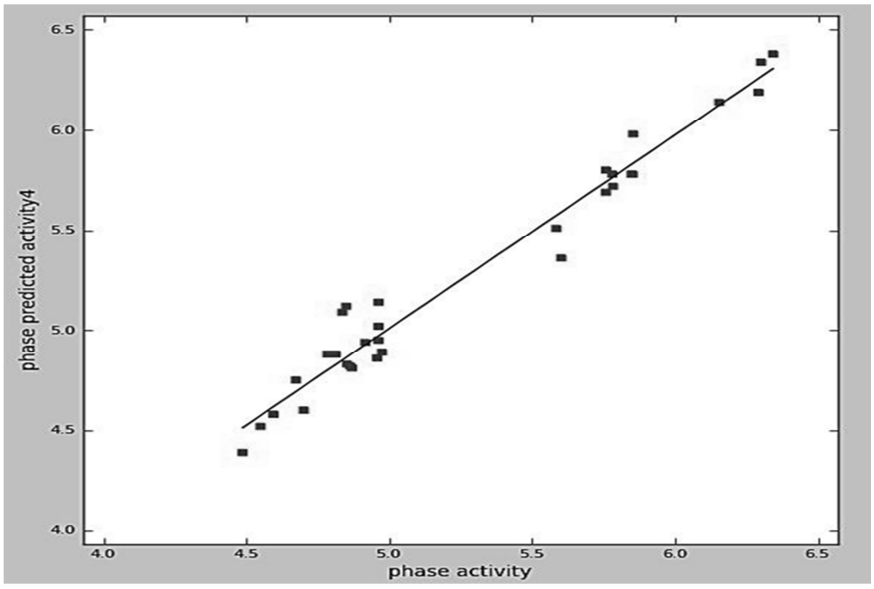

Figure 6: QSAR Plots of predicted vs actual pIC_{50} for training set ligands obtained from Field-based QSAR

REFERENCES

[1] Hughes, G. K.,Lahey, F. N.,Price, J. R.,Webb, L. J.,*Nature*.**1948**, 162, 223–224.
[2] Su, T. L., Lin, Y. W., Chou, T. C., Zhang, X., Bacherikov, V. A., Chen, C. H., Liu, L. F., Tsai, T. J., *J. Med. Chem*. **2006**, 49, 3710-3718.
[3] Kelly, J. X., Smilkstein, M. J., Brun, R., Wittlin, S., Cooper, R. A., Lane, K. D., Janowsky, A., Johnson, R. A., Dodean, R. A., Winter, R., Hinrichs, D. J., Riscoe, M. K., *Nature*. **2009,** 459, 270-273.
[4] Hyafil,F., Vergely,C., Vignoud,P. D., Perret,T. G., *Cancer Res*. **1993**, 53, 4595–4602.
[5] Walstab,A., Koester,M., Bohme,M., Keppler,D., *Br. J. Cancer.***1999**, 79, 1053–1060.
[6] Traunecker,H. C. L., Steven,M. C. G., Kerr,D. J., Ferry,D. R., *Br. J. Cancer.***1999**, 81, 942–951.
[7] Horton,J. K., Thimmaiah,K. N., Altenberg,G. A., Germain,G. S., et al., *Mol. Pharmacol*. **1997,** 52, 948–957.
[8] Kawaii, S., Tomono, Y., Katase, E., Ogawa, K., Yano, M., Takemura, Y., Ju-ichi, M., Ito, C., Furukawa H., *J Nat Prod*.**1999,** 62, 587-589.
[9] Braga, P. A., Dos Santos, D. A., Da Silva, M. F., Vieira, P. C., Fernandes, J. B., Houghton, P. J., Fang, R., *Nat Prod Res*. **2007**,21, 47-55.
[10] Svoboda,G. H., Poore,G. A., Simpson,P. J., Boder,G. B., *J. Pharm. Sci.***1966**, 55, 759–768.
[11] Chou,T. C., Wu,T. S., Tzeng,C. C., Watanabe,K. A., Su,T. L., *Phytother. Res.***1989**, 3, 237–242.
[12] Sathish,N. K., Rajendra Prasad,V. V. S., Raghavendra,N. M., Shanta Kumar,S. M., Mayur,Y. C., *Sci. Pharm.***2009**, 77, 19–32.
[13] Rajendra Prasad,V. V. S., Peters,G. J., Lemos,C., KathmannI., MayurY. C., *Eur. J. Pharm. Sci*. **2011**, 43, 217–224.
[14] Rajendra Prasad,V. V. S., VenkatRao,J., Giri,R. S., Sathish,N. K., Shanta Kumar,S.M., MayurY. C., *Chem.Biol. Interact*. **2008**, 176, 212-219.
[15] Ligprep, version 2.6.NewYork: Schro¨dinger, LLC; 2013. (http://www.schrodinger.com/LigPrep/).
[16] Phase, Version 3.5.NewYork: Schrodinger, LLC; 2013. (http://www.schrodinger.com/Phase/).
[17] Kalva, S., Vinod, D., Saleena, L. M,,*Med. Chem. Res*. **2013,** 22, 5303-5313.
[18] Rajendra Prasad, V. V. S., Deepak Reddy, G., Appaji, D., Peters, G. J., Mayur, Y. C.,.*J. Mol. Graphics Modell*.**2013**, 40, 116-124.